Journal of the European Ceramic Society 19 (1999) 737–740

PII: S0955-2219(98)00316-1
0955-2219/99/$ - see front matter

Electrical Conductivity and Nonstoichiometry in Doped $Sr_3Ti_2O_7$

Carlos Navas,[a] Harry L. Tuller[a]* and Hans-Conrad zur Loye[b]

[a]Department of Materials Science and Engineering, Massachusetts Institute of Technology, Cambridge, MA 02139, USA
[b]Department of Chemistry and Biochemistry, University of South Carolina, Columbia, SC 29208, USA

Abstract

A series of doped Ruddlesden–Popper phases, of general formula $Sr_3Ti_{2-x}M_xO_{7-\delta}$ ($M = Al, Ga, Co$), were synthesized and their electrical conductivity characterized as a function of temperature and oxygen partial pressure. For fixed-valent dopants, p-type conductivity predominates at $p(O_2) > 10^{-5}$ atm, followed by a $p(O_2)$-independent electrolytic regime, and n-type electronic conductivity at very low $p(O_2)$. The electrolytic regime exhibits activation energies in the range 1·7–1·8 eV. Doping with transition metals such as Co results in a very significant increase in total conductivity with a p-type conductivity at high $p(O_2)$. Furthermore, an apparent ionic regime at intermediate $p(O_2)$ is observed, characterized by high conductivity ($> 10^{-2}$ S/cm at 700°C) and low activation energy (0·6 eV). This interpretation is consistent with iodometric measurements as interpreted by a defect chemical model. Other measurements are in progress to confirm this conclusion. © *1999 Elsevier Science Limited. All rights reserved*

Keywords: defects, ionic conductivity, perovskites, fuel cells, sensors.

1 Introduction

Fuel cell technology has received growing attention in the past decade due to its promise of providing cleaner and more efficient energy conversion. Solid oxide fuel cells (SOFCs), in particular, are being targeted for stationary applications given their fuel flexibility and high conversion efficiencies.[1] Relatively high operating temperatures, however, require more costly designs. Materials are therefore being sought to replace the key components of the cell (electrolyte, electrodes and interconnects) with more conductive and/or interfacially active alternatives and thereby enable lower temperature operation.[2]

Layered compounds provide an important degree of flexibility in manipulating the electrical and transport properties of ionic solids. As an example, we have been able to synthesize a new family of ionic conductors based on doped Aurivillius phases with Bi as a key component element.[3,4] In an effort to extend the ionic domain of such materials to a wider range of partial pressures of oxygen, we have initiated studies on a family of layered perovskites, the so-called Ruddlesden–Popper phases[5] with general formula $A_{n+1}B_nO_{3n+1}$.[6,7] The structure is made up of n ABO_3 perovskite-like layers sandwiched between AO rock salt-type layers which, unlike the Aurivillis phases studied in our group, are lacking the $\{Bi_2O_2\}^{2+}$ layer in order to avoid the reduction problem. Furthermore, these oxides offer excellent compositional flexibility by enabling substitution of a variety of cations onto the B-site of the perovskite region. Specifically, $Sr_3M_2O_{7-\delta}$ (M = Ti, Co, Fe, Mn) have all been reported in the literature,[7–10] thereby offering the possibility of mixed conduction in $Sr_3Ti_{2-x}M_xO_{7-\delta}$ solid solutions, of interest as electrode materials.[2] In addition, fixed-valent cations such as Al^{3+} and Ga^{3+} may substitute for Ti, affording the possibility of high ionic conduction by creation of oxygen vacancies. This paper deals with the synthesis and characterization of the electrical properties of a new series of materials, of general formula $Sr_3Ti_{2-x}M_xO_{7-\delta}$ (M = Al, Ga, Co).

2 Theory

For the purposes of this study, we review the key features of the defect chemistry of an oxide with either fixed or variable valence dopants.[11] Frenkel

*To whom correspondence should be addressed. Fax: +1-617-258-5749; e-mail: hltuller@mit.edu

disorder on the oxygen sublattice can be represented in the following form, using Kroger–Vink notation

$$O_o^x \leftrightarrow O_i'' + V_o^{\bullet\bullet} \tag{1}$$

where O_o^x, O_i'' and $V_o^{\bullet\bullet}$ represent a lattice oxide ion, a doubly charged interstitial oxide ion and oxygen vacancy, respectively. We also consider electron-hole pair generation, described by

$$O \leftrightarrow e' + h^{\bullet} \tag{2}$$

as well as the equilibrium with the gas phase

$$O_o^x \leftrightarrow V_o^{\bullet\bullet} + \frac{1}{2}O_2 + 2e' \tag{3}$$

For variable-valence dopants, N_M, one describes the ionization reaction by

$$N_M^x + e' \leftrightarrow N_M' \tag{4}$$

with the further constraint that the total concentration of the dopant remains constant

$$\left[N_M^x\right] + \left[N_M'\right] = [N_M]_{\text{tot}} = N_t \tag{5}$$

The mass-action relations for eqns (1)–(4) are, respectively,

$$\left[O_i''\right]\left[V_o''\right] = K_F = K_F^o \exp(^{-}E_F/kT) \tag{6}$$

$$np = K_i = N_c N_v \exp\left(^{-}E_g/kT\right. \tag{7}$$

$$\left[V_o''\right] n P_{O_2}^{1/2} = K_R = K_R^o \exp(^{-}E_R/kT) \tag{8}$$

$$\left[N_M'\right]/\left[N_M^x\right] n = K_D = K_D^0 \exp(^{-}E_d/kT) \tag{9}$$

and finally, we consider the electroneutrality balance equation

$$n + 2\left[O_i''\right] + \left[N_M'\right] = p + 2[V_o^{\bullet\bullet}] \tag{10}$$

The above equations are commonly solved using the Brouwer approach, whereby one assumes that for a given set of T and $p(O_2)$, only one defect predominates on each side of eqn (10). For example, at high $p(O_2)$, O_i'' and $h^{\bullet}$ predominate and $N_M^x = N_t$, so that eqn (10) reduces to $2\left[O_i''\right] = p$; on the other hand, at sufficiently low $p(O_2)$, $V_o^{\bullet\bullet}$ and e' predominate and $N_M' = N_t$, so that eqn (10) is reduced to $n = 2[V_o^{\bullet\bullet}]$. With a fixed-valent dopant, four main regions with their corresponding electroneutrality equations and mass-balance relations are expected. We note that in one of these regions, $V_o^{\bullet\bullet}$ shows no $p(O_2)$ dependence and simultaneously n and p follow $p(O_2)^{-1/4}$ and $p(O_2)^{+1/4}$ dependencies, respectively. This enables one to identify the electrolytic regime.[2] In contrast, in the case of a variable-valence dopant, five such regions can theoretically be observed (Fig. 1). We note that now $V_o^{\bullet\bullet}$. predominates not only in region IV where it shows no $p(O_2)$ dependence but also in parts of region III were it follows a $p(O_2)^{-1/6}$ dependence. Likewise, it should be noted that holes exhibit a $p(O_2)$ independent regime in region II. One may distinguish the ionic regime IV from the electronic regime II by noting that the transition to an ionic regime is accompanied by a reduction of the variable-valence dopant (regions III and IV). This will be tested in our studies experimentally by iodometric titration.

3 Experimental

All materials were synthesized by the standard solid state reaction of the respective oxides or carbonates at temperatures ranging between 1250 and 1450°C. Phase purity and cell parameters were investigated using X-ray diffraction (XRD) on a Siemens D5000 diffractometer with a monochromator. Their electrical conductivities were evaluated as a function of temperature and oxygen partial pressure from the impedance spectra obtained with a Solartron 1260 impedance analyzer. The nonstoichiometry of samples quenched from 700°C under various partial pressures of oxygen was measured by titration.

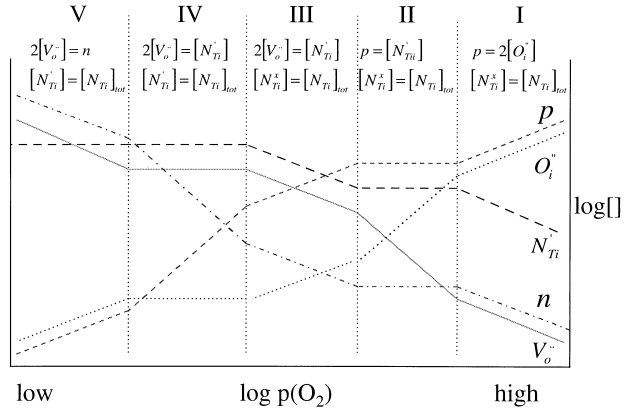

Fig. 1. Dependence of defects on $p(O_2)$ for a variable-valent dopant.

4 Results and Discussion

All samples were initially found to be single phase by XRD, and were indexed according to the tetragonal cell corresponding to the parent phase.[12] Cell parameters show a decrease in both the *a* and *c* parameters with increasing concentration of dopants as expected, due to the smaller size of all dopant cations with respect to Ti^{4+}.

Measurements of conductivity as a function of temperature in air for some fixed-valent doped samples reveal an increase in the total magnitude of the conductivity with respect to the parent, stoichiometric phase. However, this amounts to only about 1 order of magnitude, up to a value of about 10^{-3} S cm^{-1} at about 900°C for some Al and Ga-doped materials. Activation energies are similar for all samples studied and are in the range of 0·8–0·9 eV.

To determine the charge carriers responsible for conduction, we carried out measurements of conductivity as a function of oxygen partial pressure at 600, 700 and 800°C (Fig. 2).[5] These measurements for the Ga-doped material reveal three clearly delimited regions. The first extends between 10^{-5} atm < p(O_2) < 1 atm; log conductivity decreases linearly with decreasing log p(O_2), with slope of approximately +1/4, corresponding to p-type conductivity. Between 10^{-18} atm < p(O_2) < 10^{-5} atm, the conductivity is independent of p(O_2), which we interpret to be ionic conductivity. For p(O_2) < 10^{-18} atm, an increase in conductivity with decreasing p(O_2) is initiated due to n-type conduction. As expected, the magnitude of the conductivity increases with temperature while the electrolytic regime shrinks with increasing temperature. The magnitude of the ionic conductivity at 800°C is about 4×10^{-5} S cm^{-1}, while the activation energy is about 1·8 eV for these Al and Ga-doped phases.

Doping with a transition metal cation (e.g. Co) has a much more drastic effect on the conductivity. Figure 3 shows the conductivity as a function of p(O_2) at 700°C for a series of Co-doped materials. The magnitude of the conductivity increases quite dramatically with increasing dopant concentration. Here, log conductivity increases with log p(O_2) between 10^{-5} atm < p(O_2) < 1 atm with a slope of approximately + 1/6. Below this p(O_2), the conductivity is independent of p(O_2), then shows a sharp drop at low p(O_2), due to partial decomposition of the sample, as confirmed by XRD. At intermediate p(O_2), the magnitude of the conductivity increases to a value of about 5×10^{-2} S cm^{-1} at 700°C for $x = 0{\cdot}8$ Furthermore, preliminary measurements indicate that the activation energy in this regime for $x = 0{\cdot}2$ is about 0·65 eV, in contrast to about 1·8 eV for the same dopant concentration of Ga or Al. Hence, it would seem that in the Co-doped samples, electronic conduction is present at intermediate p(O_2)s. If this is the case, the transition metal cation remains in its more highly oxidized form (see Section 2). If instead it corresponds to ionic conduction (region IV), then the p-type regime that precedes this region at higher p(O_2) should be related to the reduction of the transition metal cation from its more highly oxidized form to its reduced form. To elucidate this problem, we carried out iodometric titration measurements on samples quenched from 700°C under various partial pressures of oxygen. The resulting nonstoichiometry data, plotted as a function of p(O_2), are shown in Fig. 4.

Several features about this graph stand out. First, the transition metal cation (Co) is indeed being progressively reduced as the partial pressure of oxygen is lowered. The slope of the line is also 1/6, which coincides with predictions (Fig. 1, region III) and with the slope of the conductivity in the p-type region. This feature seems to indicate, according to our defect model, that the p(O_2)-independent region is indeed ionic in nature and that the low activation energy observed in this region corresponds to ionic migration. Although

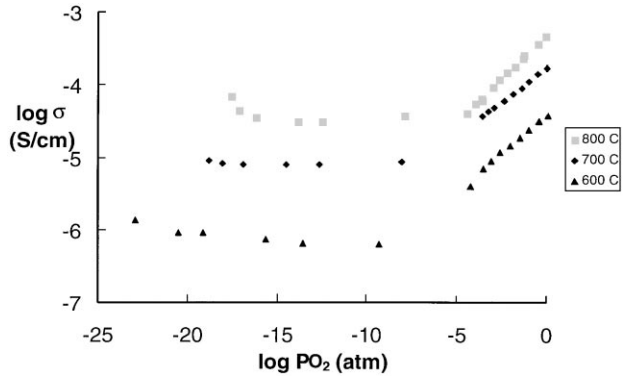

Fig. 2. Conductivity as a function of oxygen partial pressure at different temperatures for $Sr_3Ti_{1.8}Ga_{0.2}O_{6.9}$.

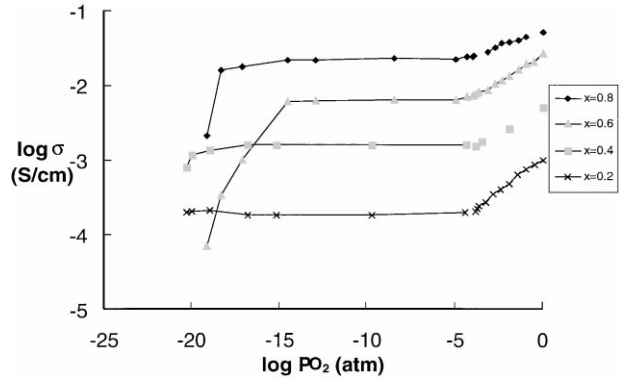

Fig. 3. Conductivity as a function of oxygen partial pressure for $Sr_3Ti_{2-x}Co_xO_{7-y}$ at 700°C.

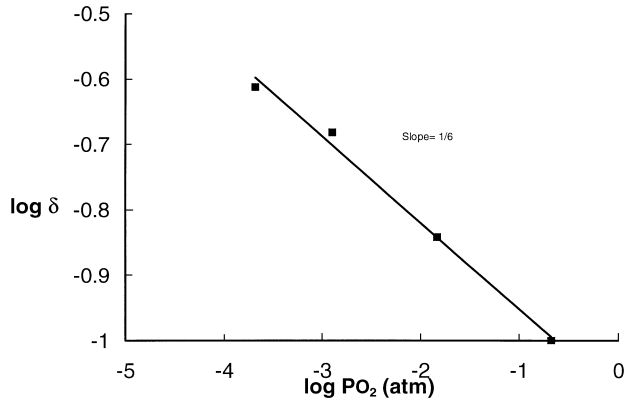

Fig. 4. Nonstoichiometry data for quenched samples of $Sr_3Ti_{1\cdot2}Co_{0\cdot8}OH_{7-\delta}$ from 700°C.

different matrix cations are known to have, at times, marked effects on ionic conductivity, the large differences observed here are surprising. Consequently, we intend to look further into this effect through future experiments including concentration cell measurements in the intermediate $p(O_2)$ regime.

The data of Fig. 4 suggests that the average oxidation state of Co is decreasing from +4 to +3 with decreasing $p(O_2)$. This is very surprising because Co(IV) compounds are rare,[13–18] and are typically synthesized using high oxygen partial pressures or electrochemical synthesis techniques. Thus, although related perovskite materials such as $La_{1-x}Sr_xCoO_{3-\delta}$ may exhibit average oxidation states for Co of up to 3·4,[19] and $SrCoO_3$ is known,[16] we did not expect our material to exhibit such a high oxidation state. In fact, $Sr_3Co_2O_{7-\delta}$ can only be made to contain a very small concentration of Co(IV) under highly oxidizing synthetic pressures.[8] In the $Sr_3Ti_{2-x}Co_xO_{7-\delta}$ system, the increase in x has to be accompanied by charge compensation through an increase in oxygen vacancies or introduction of Co^{4+}. Since the $x=2$ end member has been shown to exhibit only Co^{3+}, we expected the former compensation mechanism to take over. However, we have found otherwise after our synthesis in air. It remains unclear why Co(IV) is stabilized in this particular structure.

5 Summary

We have investigated a family of oxygen-deficient, doped Ruddlesden–Popper phases. Doping with fixed valent cations such as Al and Ga results in an increase in the total conductivity. An ionic regime is observed at intermediate $p(O_2)$, characterized by low conductivity and high activation energy. Doping with transition metals such as Co results in a very significant increase in total conductivity. Furthermore, an apparent ionic regime at intermediate $p(O_2)$ is observed, characterized by high conductivity ($>10^{-2}$ S cm^{-1} at 700°C) and low activation energy (0·6 eV). This interpretation is consistent with iodometric measurements as interpreted by a defect chemical model. Other measurements are in progress to confirm this conclusion.

Acknowledgements

The authors thank the National Science Foundation for partial support of this program under contract # DMR-9701699.

References

1. Minh, N. Q. and Takahashi, T., *Science and Technology of Ceramic Fuel Cells*. Elsevier, 1995.
2. Tuller, H. L., In *High Temperature Electrochemistry: Ceramics and Metals*, ed. F. W. Poulsen, *et al*., Risø National Laboratory: Røskilde, Denmark, 1996, p. 139–153.
3. Kendall, K. R., Thomas, J. K. and zur Loye, H. C., *Chem. Mater.,* 1995, 7(1), 50–57.
4. Kendall, K. R., Navas, C. and zur Loye, H. C., In *Materials Research Society Symposium Proceedings: Solid State Ionics IV*. ed. Nazri, G.-A., Tarascon, L-M. and Armand, M. MRS, Boston, MA; 1995, 355–360.
5. Navas, C. and zur Loye, H. C., *Solid State Ionics*, 1997, **93**, 171–176.
6. Ruddlesden, S. N. and Popper, P., *Acta Cryst.,* 1957, **10**, 538–539.
7. Ruddlesden, S. N. and Popper, P., *Acta Cryst*., 1958, **11**, 54–55.
8. Dann, S. E. and Weller, M. T., *J. Solid State Chem*., 1995, **115**, 499–507.
9. Dann, S. E., Weller, M. T. and Currie, D. B., *J. Solid State Chem*., 1992, **97**, 179–185.
10. Mizutani, *J. Chem. Soc. (Japan) Ind. Ed.,* 1970, **73**, 1097–1103.
11. Tuller, H. L., In *Nonstoichiometric Oxides*, ed. Sorensen, O. T., Academic Press: New York, 1981, 271–332.
12. Navas, C., Tuller H. L., and zur Loye, H.-C., unpublished
13. Jansen, V. M. and Hoppe, R., *Z Anorg. Allg. Chem.,* 1973, **398**, 54.
14. Jansen, V. M. and Hoppe, R., *Z Anorg. Allg. Chem.,* 1974, **408**, 75.
15. Jansen, V. M. and Hoppe, R., *Z Anorg. Allg. Chem.,* 1974, **409**, 152.
16. Bezdicka, P., Wattiaux, A., Grenier, J. C., Pouchard, M., Hagenmuller, P., *Z Anorg. Allg. Chem.,* 1993, 619, 7, and references within.
17. Liu, L. M., Lee, T. H., Qui, L., Yang, Y. L., Jacobson, A. J., *Mat. Res. Bull*., 1996, **31**, 29.
18. Yoshiasa, A, Inoue, Y, Kanamaru, E, Koto, K., *J. Solid State Chem*., 1990, **86**, 75.
19. Mineshige, A, Inaba M., Yao, T, Oguji, Z., *J. Solid State Chem*., 1996, **121**, 423–429.